Microneedle Delivery of Ophthalmic Macromolecules

Cherilyn Go
Alan Gomez
Brian Hsu
Hillary Lam

BENG 221
October 24, 2014

Table of Contents

Introduction

Since the introduction of human insulin for the treatment of diabetes, the use of biopharmaceuticals for the treatment of human disease and illness has rapidly increased [1]. Biopharmaceuticals allow for the treatment of diseases with few side effects whereas typical pharmaceuticals may be less effective or exhibit harmful side effects. One major field of medicine in which biomolecules have been making an impact is in the treatment of ocular diseases. In 2010, the number of visually impaired people worldwide was approximately 285 million, of which 39 million people were blind [2]. The most common diseases that significantly affect vision are age-related macular degeneration (AMD), diabetic retinopathy, cataracts, uveitis, keratitis, and glaucoma [3]. There already exists a number of biomolecules for ophthalmic indications approved by the FDA such as aptamer, pegatanib and ranibizumab [4], with many more in clinical trials. As the sales of ophthalmic biopharmaceuticals are expected to exceed $8 billion in 2016, there is a significant market for improvements in ophthalmic treatments [4].

In many cases, biopharmaceuticals are large molecules (macromolecules) that cannot be delivered effectively via conventional methods such as topical delivery, or eye drops. The large size of the macromolecules limits the diffusion across the layers of the ocular tissue and renders topical application ineffective (Figure 1). One common method of ophthalmic macromolecule delivery involves weekly or monthly intravitreal injections that must be performed by an ophthalmologist [5]. To maximize the effectiveness of the drug, the drug should be delivered locally to the site of action. Because the eye is small in size and has a large number of distinct tissues, targeted drug delivery to a specific tissue within the eye is especially difficult.

Figure 1. Challenges of ophthalmic macromolecule delivery [3]

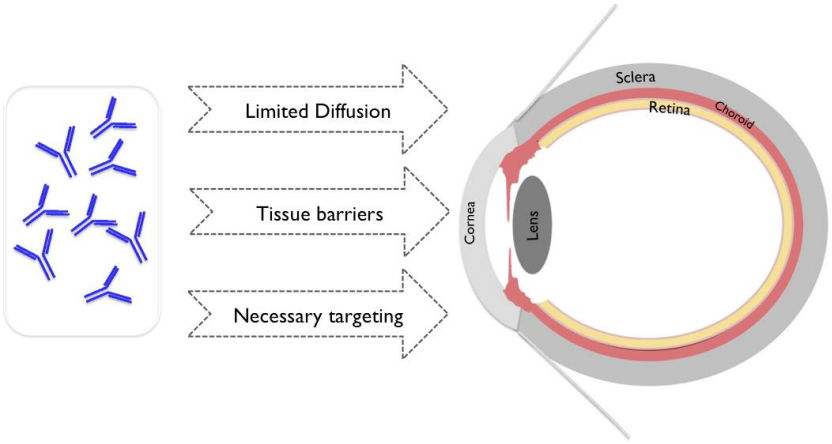

In this project, we aim to explore the use of microneedles for ophthalmic delivery of macromolecules. Drug delivery via microneedles has already been proven to be an effective delivery modality for biologics in the skin (Figure 2). Currently, transdermal microneedles are being used to deliver macromolecules such as proteins, RNA, and pDNA to the epidermis of a patient by bypassing the stratum corneum and delivering directly into the epidermis [6]. Microneedle patches are coated with a water-soluble drug solution that dissolves after insertion and diffuses into the target tissue [6]. In a similar fashion, we suggest that microneedles can be

used in ophthalmic drug delivery--more specifically, the use of microneedles to bypass the low diffusive corneal epithelial layer and to deliver macromolecules to the corneal stromal layer.

Figure 2. Example of transdermal microneedle patch (R. Prausnitz Lab)

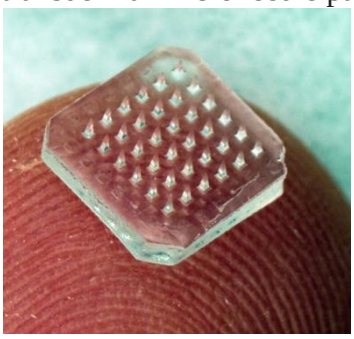

Microneedle Model

Our model demonstrates diffusion of an ophthalmic drug across the cornea via a coated microneedle. We model the diffusion as a 1-D single slab problem along the visual axis of the eye and assume that the drug is released instantaneously after insertion into the most anterior portion of the corneal stroma (posterior of the epithelial layer), as shown in Figure 3, and modeled by the impulse function in our initial conditions. After being released, the drug diffuses into the stroma and is simultaneously absorbed by the local stromal cells—the target tissue.

Our second assumption is that the diffusion of the drug is not affected by its charge or polarity. We also assume that the cornea is a flat slab and that the drug does not diffuse into the aqueous humor and cannot diffuse backwards into the epithelial layer, implemented by our zero-flux boundary conditions. The tissue porosity and absorption coefficient of the drug were taken from literature on porcine and rabbit corneal stroma, respectively [7,8]. The average thickness of the corneal stroma and epithelial layers are 50 um and 50 um, respectively [9]. The parameters of our model are summarized in Table 1. Using Fick's law of diffusion with an added term to simulate consumption of the drug, we solved the governing equation for the microneedle model to determine the concentration profile of the drug across time and space (Appendix A).

Governing Equation: $$\frac{\partial C}{\partial t} = D\frac{\partial^2 C}{\partial x^2} - \frac{\beta}{1-\varepsilon}C$$

IC: $$C(x,0) = C_0\delta(x)$$

BC: $$\frac{\partial C}{\partial x}(0,t) = 0 \qquad \frac{\partial C}{\partial x}(L,t) = 0$$

Analytical Solution: $$C(x,t) = \sum_{n=0}^{\infty} \frac{2C_0}{L}\cos\left(\frac{n\pi x}{L}\right) e^{-\left(\left(\frac{n\pi}{L}\right)^2 D + \frac{\beta}{(1-\varepsilon)}\right)t}$$

Topical Delivery Model

In order to show that microneedles are more effective in delivering macromolecules to corneal stroma, we also modeled drug delivery via topical application, or eye drops (Figure 3). In this model, the ophthalmic drug must first diffuse across the epithelial layer and then through the stroma to reach the target cells. The two layers have different diffusion coefficients, as molecules

diffuse more readily through the stroma than the epithelium. Although more accurately represented by a two-slab diffusion model, we simplified the diffusion of the drug to a lumped-parameter model. Rather than taking the average of the two diffusion coefficients, we decided to account for the difference in the diffusivity throughout the lumped parameter model by implementing a hyperbolic function into our governing equation, which should more accurately reflect the difference of the layer thicknesses.

Diffusion coefficient for lumped-parameter model:

$$D(x) = D_{epi} + \left(D_{stroma} - D_{epi}\right)\left(1 - e^{kx}\right)$$

According to this function, the diffusion coefficient is no longer a constant and now changes with respect to position within the slab. We chose an appropriate value for k so that $D_{epithelium}$ is dominant within the first 10% of the slab, while D_{stroma} is dominant within the last 90% of the slab. Because the diffusivity is a function of position, it becomes difficult to solve the governing equation analytically. Therefore, to approximate the efficacy of topical drug delivery, we used numerical methods—namely, Matlab's PDEPE and finite differences—to generate a diffusion profile.

Figure 3. Illustration of microneedle versus topical drug delivery of macromolecules

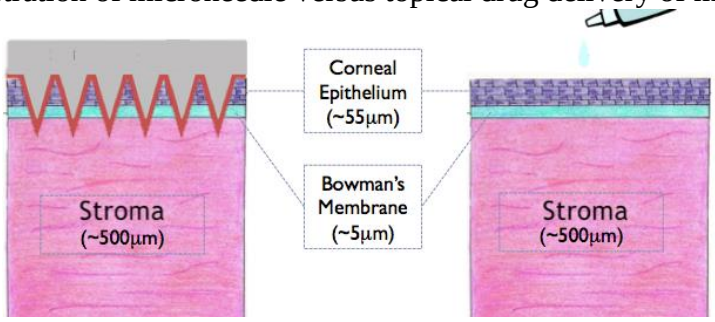

Table 1. Parameter Values and Physiological Meaning

Parameter	Model Variable	Value	Unit	Biological Meaning
Absorption rate	β	5×10^{-4}	g/s	Rate of consumption by stromal cells (binding with receptors)
Diffusion coefficient	D_{epi} D_{stroma}	2×10^{-6} 10×10^{-9}	m^2/s	How fast the drug can diffuse through a specific material
Porosity	ε	0.5	N/A	Measure of void space out of total tissue
Rate of exponential decay	k	250	N/A	Depending on relative thickness of layers, k determines whether D_{epi} or D_{stroma} dominates at a given position
Initial Drug Concentration	C_0	.1	ug/mL	
Thickness	L	500×10^{-6}	m	Tissue thickness

Results and Discussion of Microneedle Model

An analysis of the surface plots and the 2-D concentration profiles (Figures 4-12) for the analytical, finite differences, and PDEPE solutions of the microneedle drug delivery model show that all three methods approximate similar concentration profiles. (Note: All graphs display normalized concentration). From the general trend of the curves, we can see that after the first 100 seconds, all the concentration profiles tend toward a low, nearly zero value. As we have homogenous zero-flux boundary conditions, it is expected that the concentration would tend towards a steady-state value. However, our models do not reach steady-state in the amount of time we prescribed because there is a slow consumption that occurs in the tissue. Only after all of the drug is fully consumed will the concentration profile reach steady-state. In our model, it is apparent that the rate of diffusion is much more rapid than the rate of consumption.

Figures 4-6. Analytical, finite differences and PDEPE solutions as surface plots

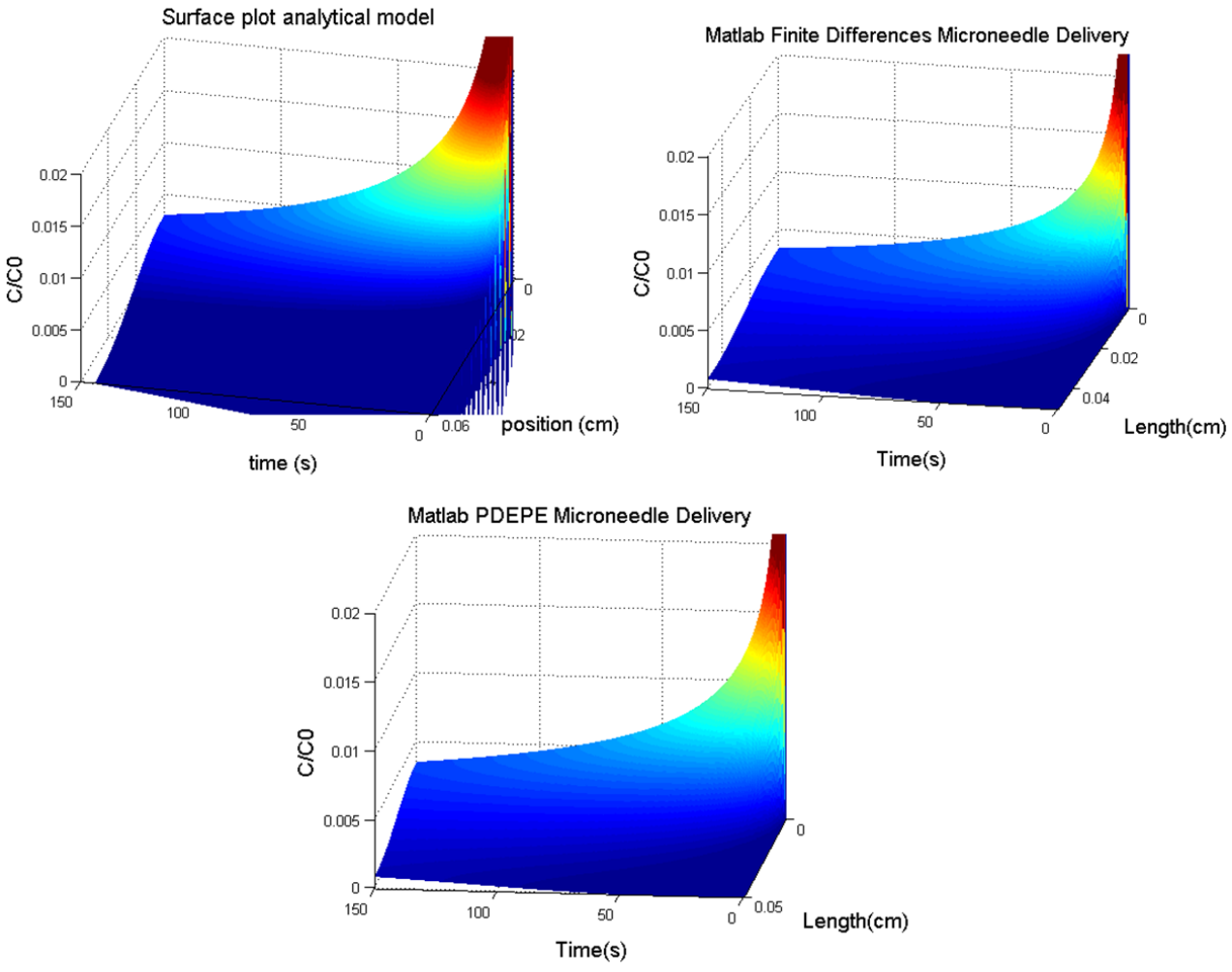

Figures 7 & 8. Analytical solution: 2-D concentration profiles for microneedle delivery

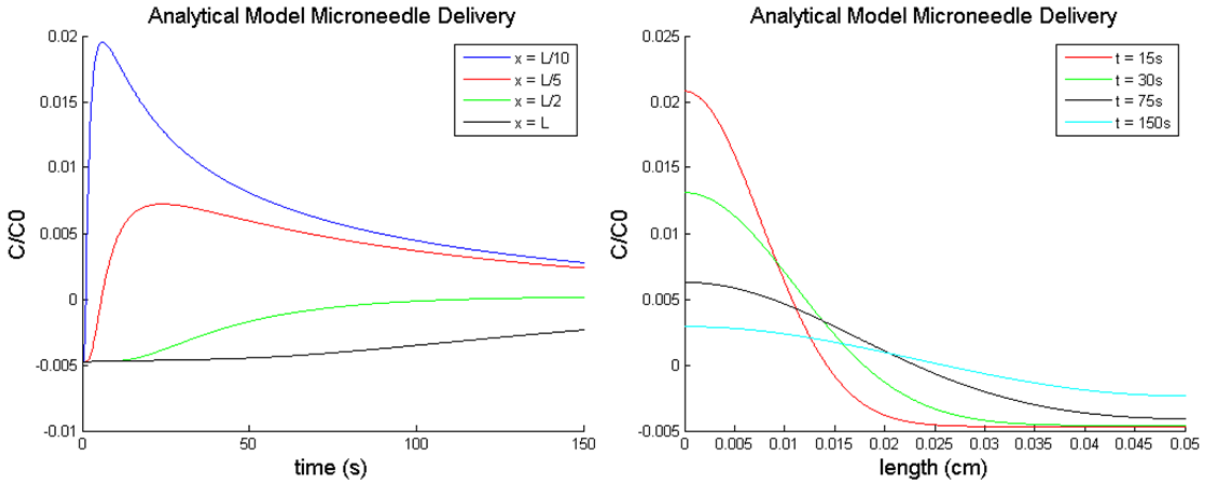

Figure 9 & 10. Finite differences: 2-D concentration profiles for microneedle delivery

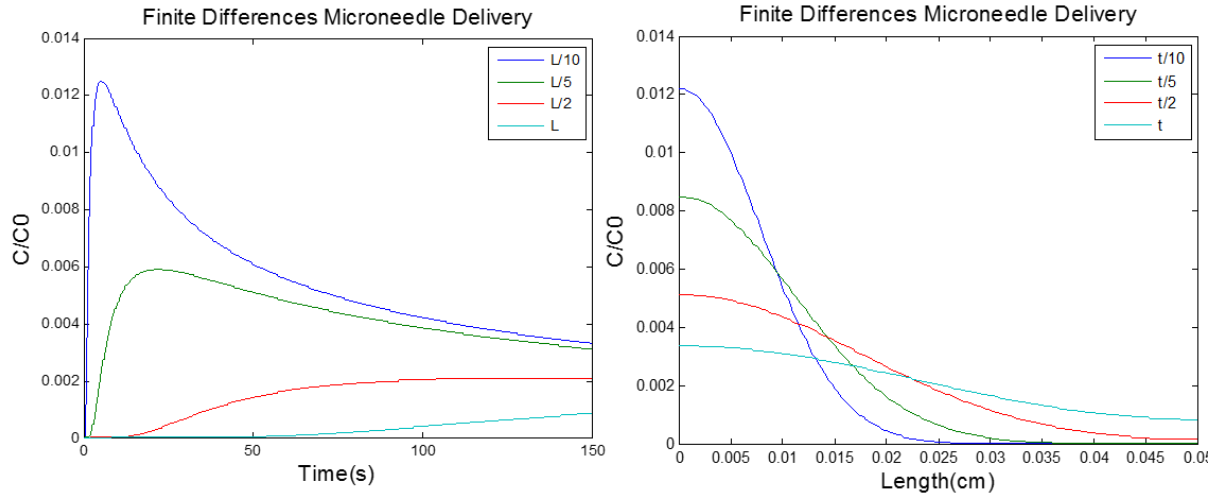

Figure 11 & 12. Matlab PDEPE: 2-D concentration profiles for microneedle delivery

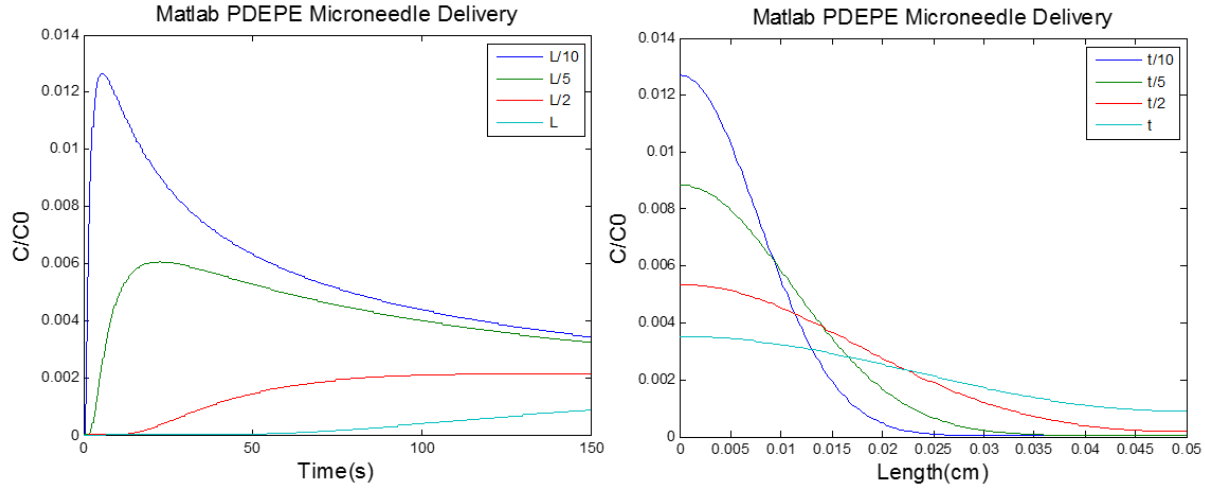

Both numerical methods approach about the same concentration values, peaking at approximately 0.012 at both length L/10 and at time t/10 (Figures 9-12); the analytical method demonstrates similar profiles, although the values were approximately 60% greater than those of the numerical solutions, as shown by the peak value of 0.02 at length L/10 and time t/10 (15 s) in Figures 7 and 8. This discrepancy may be due to the number of iterations run (n=100); a larger number of iterations may help to more accurately reflect the solution. Although the two numerical methods show very similar results, there are still slight differences in the values of each method, which can be attributed to their respective limitations.

Limitations of Analytical, Finite Differences and PDEPE Methods

Using the analytical solution, Matlab cannot implement a dirac delta function and must be approximated by an infinite summation; on the other hand, the numerical methods can implement the dirac delta function relatively well. For the analytical model, we ran 100 iterations, which ignores all the higher eigenmodes. Theoretically, to achieve the most accurate analytical solution, we would need to perform the summation over an infinite number of iterations. Although the low number of iterations saves a great amount of computation time and power, it comes at the detrimental cost of accuracy, which is evident in our model: the analytical solution begins at a negative concentration due to the oscillatory behavior from the cosine term and the position we chose to observe.

One major limitation of the finite differences method is that it is intolerant of changes to dt and dx; reducing dx causes the step size to increase significantly, which requires a two-fold decrease in dt to compensate. Thus, in order to achieve good spatial resolution, dx and dt must be reduced, which causes an increase in number of time steps and computation time.

The greatest limitation of PDEPE is the number of iterations it can run before requiring excessive computational time and power, similar to the limitations of the analytical and finite differences method. Amongst the three methods, given a discrete amount of computational time and power, PDEPE seemed to provide us with an accurate approximation of the solution with the least amount of effort needed for optimization (unlike the required optimization of the number of summations for the analytical solution, and of the step size for the finite differences method).

Results and Discussion of Topical Delivery Model

After verifying that the numerical methods provided good approximations of the microneedle delivery profiles, we can now utilize these same methods to approximate the solution to the governing equation of the topical delivery lumped-parameter model without solving it analytically. Using the topical delivery model, limitations of the finite differences methods become more apparent and significant. As seen previously, the finite differences method is intolerant in of changes to parameter values. For example, if D_{stroma} is less than $D_{epithelium}$, the step size becomes a negative term, causing oscillations centered at zero. The finite difference method is also limited by its nature: because the step size is a function of diffusivity, and in turn the diffusivity of the lumped-parameter model is a function of position, the step size changes with each iteration. With each iteration, errors accumulate, providing us with an inaccurate approximation of the solution (Figures 13-16). Therefore, in order to compare the microneedle delivery to the topical delivery, solely PDEPE was used.

Figures 13 & 14. Finite differences: 2-D concentration profiles for topical delivery

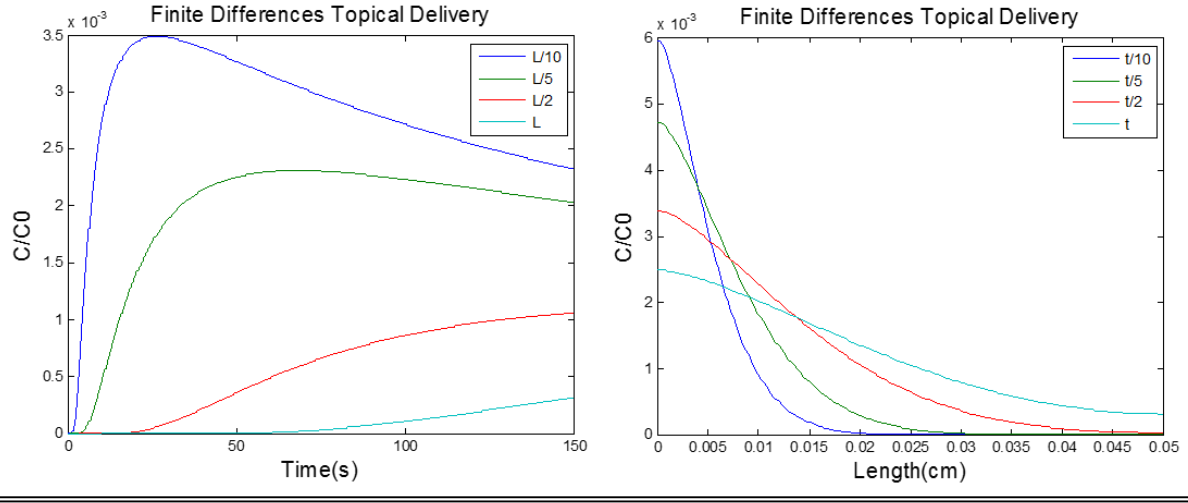

Figures 15 & 16. Matlab PDEPE solutions 2-D concentration profiles for topical delivery

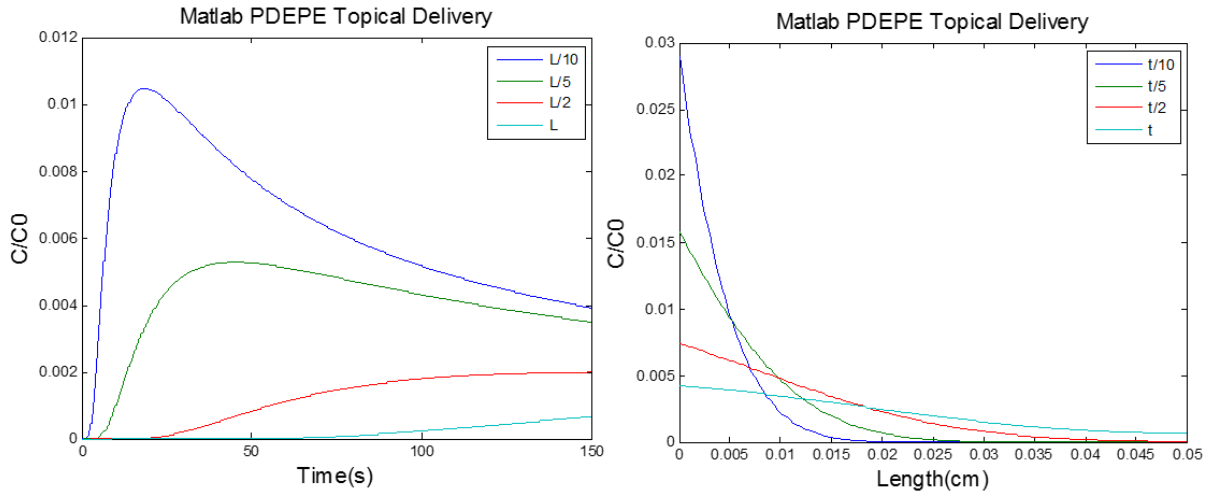

An analysis of the graphical and numerical data using PDEPE allows us to compare the efficacy of microneedle (Figures 11 & 12) and topical drug delivery (Figures 15 & 16) at varying times and positions. For the concentration versus time plots, the concentration is higher in the topical model at a given position, so we can infer that a greater concentration of the drug has penetrated deeper into the tissue for the microneedle delivery. In the concentration versus position plots, the trend of the curve determines how far the drug has diffused into the tissue. With the topical model, the curve is steeper than its microneedle counterpart and has diffused over a shorter length in the same period of time. These results are expected because the drug must first diffuse through a layer with a much lower diffusivity coefficient.

Model Limitations and Adjustments

Due to the mathematical simplifications and boundary conditions applied, the models for microneedle patch and topical drug delivery require further work to simulate experimental conditions. Limitations within our mathematical model resulted from the chosen diffusion coefficients, numerical method setup, and the lumped parameter characteristics. The model also ignored biological factors that would affect drug delivery.

The concentration and time scale vary depending on the diffusion coefficient chosen. Initially, we modeled our macromolecule on unoprostone, an ocular drug typically delivered via eye drops. As there was little data on unoprostone's diffusion coefficient, we used the diffusion coefficient in corneal tissue of a molecule with similar molecular weight. However, the value is dependent not only on size, but shape and interactions with the solvent [10]. Moreover, the diffusion coefficient becomes a function of location in the hyperbolic model, whereas normally it is a function of the variables discussed previously. A two-slab model with distinct diffusion coefficients, diffusion equations, and boundary conditions would solve this problem, as well as consumption in the epithelial tissue. Using a lumped-parameter model causes consumption to occur in both layers, though the drug targets corneal tissue only. The diffusion equation for the two-slab model would use Fick's law of diffusion and the diffusion with consumption. Without uptake in the epithelial layer, the diffusion profile would be expected to have a small time delay before concentration decreases due to the consumption term.

When creating our model, we assumed that the cornea is a flat slab, but it is actually a curved layer that varies in thickness between different people. In addition, eye conditions such as astigmatism cause it to be uneven in thickness. A two or three-dimensional model would provide a more accurate look of diffusion in the curved surface. Future work would focus on translating our model from one-dimensional diffusion to a three-dimensional analysis that includes characteristics of the microneedle patch, such as flux due to timed release and needle geometry, spacing, width, number, and length.

Conclusion

Using analytical and numerical methods, we have analyzed the diffusion of macromolecules into the cornea for two modalities of drug delivery: topical eye drops and microneedle patch. Our goal was to compare the rate of diffusion between the two systems, as the optimal system would diffuse through the cornea rapidly and bind to corneal stroma tissue. As we hypothesized, the microneedles (one-slab model) delivered the drug at a faster rate than the topical application (lumped-parameter model), as it bypassed the epithelial layer with a lower diffusivity. Though the PDEPE and finite differences model show slight variation in magnitude for the microneedle model, the general shape of the 2-D curves and surface plot exhibit the same trends. A side-by-side comparison of the topical and microneedle drug delivery models using the PDEPE method show that the macromolecule diffuses faster in the latter model. Since we have greatly simplified the microneedle patch, a more complex model with more realistic assumptions would be needed to further study the diffusion profile in vivo. However, with the apparent improvement in drug delivery efficacy via microneedles, this may be a fast and pain-free method used in the future to treat ophthalmic conditions.

References

[1] Ryu, Jae Kuk, Hyo Sun Kim, and Doo Hyun Nam. "Current status and perspectives of biopharmaceutical drugs." *Biotechnology and Bioprocess Engineering* 17.5 (2012): 900-911.

[2] Pascolini, Donatella, and Silvio Paolo Mariotti. "Global estimates of visual impairment: 2010." *British Journal of Ophthalmology* (2011): bjophthalmol-2011.

[3] Kim, Yoo Chun, et al. "Ocular delivery of macromolecules." *Journal of Controlled Release* 190 (2014): 172-181.

[4] Syed, Basharut A., James B. Evans, and Leonard Bielory. "Wet AMD market."*Nature Reviews Drug Discovery* 11.11 (2012): 827-827.

[5] El Sanharawi, M., et al. "Protein delivery for retinal diseases: from basic considerations to clinical applications." *Progress in retinal and eye research*29.6 (2010): 443-465.

[6] Kim, Yeu-Chun, Jung-Hwan Park, and Mark R. Prausnitz. "Microneedles for drug and vaccine delivery." *Advanced drug delivery reviews* 64.14 (2012): 1547-1568.

[7] Xiao, Jianhui, et al. "Construction of the recellularized corneal stroma using porous acellular corneal scaffold." *Biomaterials* 32.29 (2011): 6962-6971.

[8] Kashiwagi, Kenji, Yoko Iizuka, and Shigeo Tsukahara. "Metabolites of isopropyl unoprostone as potential ophthalmic solutions to reduce intraocular pressure in pigmented rabbits." *The Japanese Journal of Pharmacology* 81.1 (1999): 56-62.

[9] Doughty, Michael J., and Mohammed L. Zaman. "Human corneal thickness and its impact on intraocular pressure measures: a review and meta-analysis approach." *Survey of ophthalmology* 44.5 (2000): 367-408.

[10] Zhang, Wensheng, Mark R. Prausnitz, and Aurélie Edwards. "Model of transient drug diffusion across cornea." *Journal of Controlled Release* 99.2 (2004): 241-258.

APPENDIX A. Analytical Solution

$$\frac{\partial C}{\partial t} = D\frac{\partial^2 C}{\partial x^2} - \frac{\beta}{1-\varepsilon}C$$

$$I.C.: C(x,0) = C_0\delta(x)$$

$$B.C.: \frac{\partial C}{\partial x}(0,t) = 0$$

$$\frac{\partial C}{\partial x}(L,t) = 0$$

$$C(x,t) = X(x) * T(t)$$

$$\frac{\partial (X(x)*T(t))}{\partial t} = D\frac{\partial^2 (X(x)*T(t))}{\partial x^2} - \frac{\beta}{1-\varepsilon}(X(x)*T(t))$$

$$X(x)\frac{dT}{dt} = D*T(t)\frac{d^2X}{dx^2} - \frac{\beta}{1-\varepsilon}X(x)*T(t)$$

$$\frac{dT}{dt} = D\frac{T(t)}{X(x)}\frac{d^2X}{dx^2} - \frac{\beta}{1-\varepsilon}T(t)$$

$$\frac{dT}{dt} + \frac{\beta}{1-\varepsilon}T(t) = D\frac{T(t)}{X(x)}\frac{d^2X}{dx^2}$$

$$\frac{1}{DT(t)}\frac{dT}{dt} + \frac{\beta}{D(1-\varepsilon)} = \frac{1}{X(x)}\frac{d^2X}{dx^2} = -\lambda$$

$$\frac{1}{X(x)}\frac{d^2X}{dx^2} = -\lambda$$

$$\frac{d^2X}{dx^2} + \lambda X(x) = 0$$

$$X(x) = C_2\cos\left(\sqrt{\lambda}x\right) + C_3\sin\left(\sqrt{\lambda}x\right)$$

$$X'(x) = -\sqrt{\lambda} * C_2\sin\left(\sqrt{\lambda}x\right) + \sqrt{\lambda} * C_3\cos\left(\sqrt{\lambda}x\right)$$

$$X'(0) = 0 = 0 + \sqrt{\lambda} * C_3$$
$$C_3 = 0$$

$$X'(x) = -\sqrt{\lambda} * C_2\sin\left(\sqrt{\lambda}x\right)$$

$$X'(L) = 0 = -\sqrt{\lambda} * C_2\sin\left(\sqrt{\lambda}x\right)$$

$$\sin\left(\sqrt{\lambda}L\right) = 0$$
$$L\sqrt{\lambda} = n\pi$$
$$\lambda = (\frac{n\pi}{L})^2$$
$$X(x) = C_2 \cos\left(\frac{n\pi x}{L}\right)$$

$$\frac{1}{DT(t)}\frac{dT}{dt} + \frac{\beta}{D(1-\varepsilon)} = -\lambda$$
$$\frac{dT}{dt} = -(\lambda D + \frac{\beta}{(1-\varepsilon)})T(t)$$
$$\frac{1}{T(t)}dT = -(\lambda D + \frac{\beta}{(1-\varepsilon)})dt$$
$$T(t) = C_1 e^{-(\lambda D + \frac{\beta}{(1-\varepsilon)})t}$$

$$C(x,t) = X(x) * T(t)$$

$$C(x,t) = C_2 \cos\left(\frac{n\pi x}{L}\right) C_1 e^{-(\lambda D + \frac{\beta}{(1-\varepsilon)})t}$$

$$C(x,t) = C_n \sum_{n=0}^{\infty} \cos\left(\frac{n\pi x}{L}\right) e^{-\left(\lambda D + \frac{\beta}{(1-\varepsilon)}\right)t}$$

$$I.C.: C(x,0) = C_0\delta(x)$$

$$C_n = C_0 \frac{\int_0^L \delta(x)\cos(\frac{n\pi x}{L})\,dx}{\int_0^L \cos(\frac{n\pi x}{L})\cos(\frac{n\pi x}{L})dx}$$

$$C_n = \frac{2C_0}{L}$$

$$C(x,t) = \sum_{n=0}^{\infty} \frac{2C_0}{L} \cos\left(\frac{n\pi x}{L}\right) e^{-\left((\frac{n\pi}{L})^2 D + \frac{\beta}{(1-\varepsilon)}\right)t}$$

APPENDIX B. Matlab code for analytical model

```
% Specifies parameters used in the analytical solution
B = 0.0005;
e = 0.5;
D = 2e-6;
L = .05;
C0 = 0.1;

% Defines boundaries for time and distance and creates mesh that the
% analytical solution will be generated from
steps = 1000;
x = linspace(0, L, steps);
t = linspace(0, 150, steps);
[x, t] = meshgrid(x, t);

% Generates the datapoints of the analytical solution
n = 0;
c = C0 * exp((-((n*pi/L)^2)*D-(B/(1-e))).*t) .* ...
    (cos(((n*pi/L)).*x));
tic;
for n = 1 : 100
    c = c + (2*C0/L) * exp((-((n*pi/L)^2)*D-(B/(1-e))).*t) .* ...
    (cos(((n*pi/L)).*x));
end
toc;

% Normalizes data
c = c /(n*2*C0/L);

% Generates 3D surface plot
surf(t, x, c, 'EdgeColor', 'none');
caxis([0 .02]);
zlim([0 0.02]);
xlabel('time (s)', 'fontsize', 14);
ylabel('position (cm)', 'fontsize', 14);
zlabel('C/C0', 'fontsize', 14);
title('Surface plot analytical model', 'fontsize', 15);

% Generates 2D plot of concentration with respect to position
figure
hold on
plot(t(:, 1), c(:, 100)');
plot(t(:, 1), c(:, 200)', 'r');
plot(t(:, 1), c(:, 500)', 'g');
plot(t(:, 1), c(:, 1000)', 'k');
hold off
legend('t = 15s', 't = 30s', 't = 75s', 't = 150s');
xlabel('time (s)', 'fontsize', 14);
ylabel('C/C0', 'fontsize', 14);
title('Analytical Model Microneedle Delivery', 'fontsize', 14);

% Generates 2D plot of concentration with respect to time
figure
```

```
hold on
plot(x(1, :), c(100, :)', 'r');
plot(x(1, :), c(200, :)', 'g');
plot(x(1, :), c(500, :)', 'k');
plot(x(1, :), c(1000, :)', 'c');
hold off
legend('t = 15s', 't = 30s', 't = 75s', 't = 150s');
xlabel('length (cm)', 'fontsize', 14);
ylabel('C/C0', 'fontsize', 14);
title('Analytical Model Microneedle Delivery', 'fontsize', 14);
```

APPENDIX C. Matlab code for numerical methods

```
clear all;
close all;
clc;

% Diffusion coefficients of corneal stroma and epithelium
global D1 D2 C0 B eps L tf R k i
D1=2e-6; %corneal stroma
D2=10e-9; %epithelial layer
C0=.1; %initial concentration @ x=0, t=0
B=.0005; %absorption rate
eps=0.5; %porosity
L=.05;
tf=150;
R=B/(1-eps);
k=150;

i=2;   % if i=1 run 1-slab if 1=2 then 2-slab

% Step size
dx=0.00025;
dt=.015;

% Domain
xmesh=0:dx:L;
tmesh=0:dt:tf;

% Finite element method initiation of variables for 1 slab
nx=length(xmesh);
nt=length(tmesh);
N1=D1*dt/(dx^2);
a=R*dt;
C1=zeros(nt,nx);
C2=zeros(nt,nx);
C1(1,:)=C0*(xmesh == 0);
C2(1,:)=C0*(xmesh == 0);

% Finite element method initiation of variables for 1 slab

if i==1

for t=1:(nt-1)
    for x=2:(nx-1)
        C1(t+1,x)=(1-a)*C1(t,x)+N1*(C1(t,x-1)-2*C1(t,x)+C1(t,x+1));
    end
    C1(t+1,1)=C1(t+1,2);
    C1(t+1,nx)=C1(t+1,nx-1);
end
C1=C1/C0; %normalized

C1p = pdepe(0,@pdefun,@ic,@bc,xmesh,tmesh);
C1p=C1p/C0;
```

```
figure (1)
plot(tmesh,C1(:,floor(nx/10)),tmesh,C1(:,floor(nx/5)),tmesh,C1(:,floor(nx/2))
,tmesh,C1(:,floor(nx)));
title('Finite Differences Microneedle Delivery','FontSize',14)
xlabel('Time(s)','FontSize',14)
ylabel('C/C0','FontSize',14)
legend('L/10','L/5','L/2','L')

figure(2)
plot(tmesh,C1p(:,floor(nx/10)),tmesh,C1p(:,floor(nx/5)),tmesh,C1p(:,floor(nx/
2)),tmesh,C1p(:,floor(nx)));
title('Matlab PDEPE Microneedle Delivery','FontSize',14)
xlabel('Time(s)','FontSize',14)
ylabel('C/C0','FontSize',14)
legend('L/10','L/5','L/2','L')

figure (3)
plot(xmesh,C1(floor(nt/10),:),xmesh,C1(floor(nt/5),:),xmesh,C1(floor(nt/2),:)
,xmesh,C1(floor(nt),:));
title('Finite Differences Microneedle Delivery','FontSize',14)
xlabel('Length(cm)','FontSize',14)
ylabel('C/C0','FontSize',14)
legend('t/10','t/5','t/2','t')

figure (4)
plot(xmesh,C1p(floor(nt/10),:),xmesh,C1p(floor(nt/5),:),xmesh,C1p(floor(nt/2)
,:),xmesh,C1p(floor(nt),:));
title('Matlab PDEPE Microneedle Delivery','FontSize',14)
xlabel('Length(cm)','FontSize',14)
ylabel('C/C0','FontSize',14)
legend('t/10','t/5','t/2','t')

figure(5)

H2=surf(tmesh,xmesh,C1p')
title('Matlab PDEPE Microneedle Delivery','FontSize',14)
xlabel('Time(s)','FontSize',14)
ylabel('Length(cm)','FontSize',14)
zlabel('C/C0','FontSize',14)
set(H2, 'linestyle', 'none')
axis([0 tf 0 L 0 .02 0 1])
caxis([0 .02])



else
for t=1:(nt-1)
    for x=2:(nx-1)
        C2(t+1,x)=(1-a)*C2(t,x)+(dt/(dx^2))*(D2+(D1-D2)*(1-exp(-
k*x*dx)))*(C2(t,x+1)-2*C2(t,x)+C2(t,x-1));

    end
    C2(t+1,1)=C2(t+1,2);
    C2(t+1,nx)=C2(t+1,nx-1);
end
```

```
C2=C2/C0; %normalized
C2p = pdepe(0,@pdefun,@ic,@bc,xmesh,tmesh);
C2p=C2p/C0;

figure (1)
plot(tmesh,C2(:,floor(nx/10)),tmesh,C2(:,floor(nx/5)),tmesh,C2(:,floor(nx/2))
,tmesh,C2(:,floor(nx)));
title('Finite Differences Topical Delivery','FontSize',14)
xlabel('Time(s)','FontSize',14)
ylabel('C/C0','FontSize',14)
legend('L/10','L/5','L/2','L')

figure(2)
plot(tmesh,C2p(:,floor(nx/10)),tmesh,C2p(:,floor(nx/5)),tmesh,C2p(:,floor(nx/
2)),tmesh,C2p(:,floor(nx)));
title('Matlab PDEPE Topical Delivery','FontSize',14)
xlabel('Time(s)','FontSize',14)
ylabel('C/C0','FontSize',14)
legend('L/10','L/5','L/2','L')

figure (3)
plot(xmesh,C2(floor(nt/10),:),xmesh,C2(floor(nt/5),:),xmesh,C2(floor(nt/2),:)
,xmesh,C2(floor(nt),:));
title('Finite Differences Topical Delivery','FontSize',14)
xlabel('Length(cm)','FontSize',14)
ylabel('C/C0','FontSize',14)
legend('t/10','t/5','t/2','t')

figure (4)
plot(xmesh,C2p(floor(nt/10),:),xmesh,C2p(floor(nt/5),:),xmesh,C2p(floor(nt/2)
,:),xmesh,C2p(floor(nt),:));
title('Matlab PDEPE Topical Delivery','FontSize',14)
xlabel('Length(cm)','FontSize',14)
ylabel('C/C0','FontSize',14)
legend('t/10','t/5','t/2','t')

figure(5)
H2=surf(tmesh,xmesh,C2p')
title('Matlab PDEPE Topical Delivery','FontSize',14)
xlabel('Time(s)','FontSize',14)
ylabel('Length(cm)','FontSize',14)
zlabel('C/C0','FontSize',14)
set(H2, 'linestyle', 'none')
axis([0 tf 0 L 0 .02 0 1])
caxis([0 .02])

end


function [c, f, s] = pdefun(x, t, u, DuDx)
global  D1  R i D2 k

if i==1

c = 1;
```

```
f = D1 * DuDx;
s = -R*u;

else


c = 1;
f = (D2+(D1-D2)*(1-exp(-k*x)))*DuDx;
s = -R*u;

end

end


function u0 = ic(x)
global C0
u0 = C0 * (x==0); %assumed instantaneous release


function [pl, ql, pr, qr] = bc(xl, ul, xr, ur, t)
pl = 0; %flux = 0 on needle side
ql = 1; %flux = 0 on needle side
pr = 0; %c = 0 on corneal end
qr = 1; %flux = 0 on corneal end
```